Integrated facies analysis, magnetic susceptibility and sea-level fluctuations in the Frasnian (Upper Devonian) of the NW Algerian Sahara

Abdessamed Mahboubi, Jean-Jacques Cornee, Raimund Feist, Pierre Camps, Catherine Girard

Integrated facies analysis, magnetic susceptibility, and sea-level fluctuations in the Frasnian (Upper Devonian) of the NW Algerian Sahara

ABDESSAMED MAHBOUBI[*], JEAN-JACQUES CORNEE[†], RAIMUND FEIST[*], PIERRE CAMPS[†]& CATHERINE GIRARD[*]

[*] Institut des Sciences de l'Evolution, Université de Montpellier, CNRS, IRD, CC064, Place Eugène Bataillon, Montpellier Cedex 05 (France)

[†] Géosciences Montpellier, CNRS and Université de Montpellier, Place Eugène Bataillon, 34095 Montpellier Cedex 05 (France)

*Corresponding author: (email: jean-jacques.cornee@gm.univ-montp2.fr)
Phone (+33 4 67 14 36 35)

Abstract: Changes in palaeoenvironment are comparatively investigated in two representative Frasnian sections of NW Algerian Sahara integrating sedimentology, magnetic susceptibility, and conodont biofacies. The Ben Zireg section is characterized by condensed, and ferruginous calcareous deposits, whereas in the South Marhouma section the sedimentation rate is high, dominated by muddy nodular limestones with several hypoxic shale intervals. In both sections, sediments were mostly emplaced on pelagic outer ramps below the limit of storm wave-base, evolving in time from proximal to distal setting.

Investigations on temporal evolution of facies and MS data permits a brought first estimate of the local sea-level trends to be made in north-western Algeria. These trends match the overall long-term rise of sea-level recognized worldwide from Frasnian Zone 5 onward. Outstanding positive excursions of the sea-level curve related to the *semichatovae* transgression as well as to the late Frasnian transgression prior to the Upper Kellwasser event can be established in this area. Whereas the sharp regression of sea-level at the Upper Kellwasser level can be confirmed with our data, no particular trend is depicted at the transition of conodont zones 11 to 12 where the presence of the Lower Kellwasser level has not been clearly recognised so far.

Keywords: Frasnian, Algerian Sahara, facies, magnetic susceptibility, sea-level

1. Introduction

The Frasnian stage in the Late Devonian is outstanding in the occurrence of one of the major sea-level rises in the Paleozoic (Haq & Shutter 2008), which culminated in spreading of basinal anoxic waters that eventually triggered the global biotic turnover at the terminal Frasnian Upper Kellwasser Event (Hallam & Wignall 1999). This long-term eustatic rise was documented mainly in Laurussia (e.g. Johnson, Klapper & Sandberg, 1985; Johnson & Sandberg, 1988; Alekseev, Konokova & Nikishin, 1996; Narkiewicz ,1988), and in South China (Chen & Tucker 2003). On the African Gondwana margin, after preliminary records from the Moroccan Anti-Atlas (Wendt & Belka 1991), only one accurate sea-level curve was recently provided (Dopieralska, Belka, & Walczak, 2016).

In this contribution we focus on Late Devonian facies and sea level fluctuations in the Algerian Sahara, by integrating results from two representative Frasnian sections of different marine palaeoenvironmental settings: the South Marhouma section and the Ben Zireg section (Fig. 1a). Indeed, this area is still poorly known in comparison to time-equivalent North America and European regions. Analyses of lithofacies, magnetic susceptibility and conodont biofacies were performed to depict changes in the depositional environment and sea level through time. The main objective of this study is first to determine whether observed changes and trends occur concomitantly in different settings of the region, and, secondly, to propose a first order relative sea-level curve through the Frasnian that can be compared with data from other continental entities. As such it aims to compare fluctuations in sea level with those depicted by Dopieralska, Belka, & Walczak. (2016) in the neighboring Tafilalet region and with the global trends in North America (Johnson, Klapper & Sandberg, 1985; Johnson & Sandberg,1988).

2. Geological setting

The Algerian Sahara is part of the North-Gondwana epicontinental margin between the Maghrebian Variscan belt to the North and the West African craton to the South (Fig. 1a). This domain was moderately affected by the Variscan deformation. The South Marhouma section is located in the intracratonic Ougarta basin that is bordered to the south by a Precambrian shield. This basin was a strongly subsiding trough filled with continental and marine Ordovician through Carboniferous

sediments, up to 10km in thickness and slightly deformed by Variscan compressional movements (Donzeau, 1974). In the northern part of the basin Upper Devonian deposits are well exposed. At least 75 m of Frasnian sediments are continuously outcropping in the South Marhouma section (coordinates: 29°57'31. 6''N, 002°06'07.8''W) (Fig. 1b). The succession comprises mudrock deposits (shales and marls) containing argillaceous micritic nodules, and, at its top, black shales that correspond to the Upper Kellwasser horizon. Goniatites from this area were described by Petter (1952) & Göddertz (1987), trilobites by Feist, Mahboubi & Girard (2016) and ichnological analyses by Bendella & Ouali (2014). The first conodont research was conducted by Mahboubi & Gatovsky (2014). It revealed a rather moderate yield of often insignificant conodont elements (less than 10 conodonts per kg in most samples) preventing a fine-scaled biostratigraphy to be established. However, the presence of a restricted number of conodont zones, i.e. FZ 5, 11, 12 and 13 were recognized with confidence, whereas zones 6-7 and 8-10 remain undifferentiated. Many dark shale intervals, notably at the base of the succession (FZ 1-4?) and in the uppermost part, did not provide any conodonts. Presently we rely on these poor data that only permit an incomplete zonation to be established at Marhouma.

In contrast to the high sedimentation rates in the Ougarta trough, these were much lower in the Bechar region at some 300 km further to the N. Here, Upper Devonian deposits represent condensed carbonate successions punctuated by hiatuses (Weyant, 1988). The Frasnien succession is most complete in the Ben Zireg section (coordinates: 31° 54'39. 4'' N, 001° 47' 58.8'' W), on the steep southern flank of an acute anticlinal structure. Conodont based biostratigraphy revealed a late Givetian through early Frasnian hiatus, superseded by a complete sequence where all conodont zones from FZ 5 to the Frasnian-Famennian boundary were recognized (Mahboubi *et al*. 2015). At the top of the succession a marker bed of typical Kellwasser facies is developed. This zonation is used in in our present study.

3. Material and Methods

Samples of hard rock were collected in intervals ranging from 0.2 to 2 m, depending on the thickness of the soft shale intercalations. Forty and sixty thin-sections were prepared from rock samples both from the South Marhouma and Ben Zireg sections, in order to to analyze petrofacies and fabrics. Microfacies descriptions follow Dunham

(1962) for carbonate rocks and Schieber (1989) for black shales. The identified facies were interpreted and related to a depositional environment setting according to Wright & Burchette (1996), Flügel (2004) and Pas *et al*. (2013; 2014). Photographs were taken with an integrated Olympus digital camera and with a scanning electron microscope (JEOL 5600).

Magnetic susceptibility measurements were performed on 90 and 54 samples in the South Marhouma and Ben Zireg sections, respectively, for preliminary investigation. Various lithologies have been measured (shales, arenaceous and carbonate rocks). In the laboratory, samples were cleaned from iron coatings prior to weighting with a highly accurate balance (precision of 0.01g). Measurements were performed with a Bartington susceptibility meter (MS-2). The unit of measure is expressed in $x10^{-7}$ m^3 kg^{-1}.

4. Results and interpretations

4.a. Lithostratigraphy

4.a.1. Ben Zireg section

The measured section is 26.6 m thick (Fig. 2). It includes five units (Units 1 – 5) extending from the middle Frasnian to the early Famennian (Mahboubi *et al*., 2015). The succession is dominated by rhythmic fine-grained carbonates.

Unit 1 belongs to Frasnian Zone 5 (FZ 5) just above a depositional hiatus during the early Frasnian. This Unit is characterized by ochre, sometimes brecciated, cherty beds with convolute-lamination (Fig. 3a). Thin iron-hydroxide coatings are displayed at the top of the unit.

Unit 2 belongs to FZ 6. It consists of greyish to brownish massive limestone beds, centimeters to decimeters in thickness, intercalated by mm to cm thick argillaceous limestone beds that display discrete nodular structures (Fig. 3b).

Unit 3 belongs to the interval ranging from FZ 7 to the top of FZ 11. It is characterized by well-bedded ferruginous and argillaceous limestones frequently coated by hardground films. The limestone beds are often wackstone with abundant pelagic microfauna (tentaculites and entomozoan crustaceans) associated with sparse euhedral pyrites and some phosphate grains. The amount of nodular structures

increases progressively upward and they are mostly related to pressure-dissolution surfaces.

Unit 4 belongs to FZ 12. It is characterized by yellowish, massive, pseudo-nodular, clay-rich limestones sometimes interbedded with thin blackish shales. The limestones are mudstone to wackstone with sparse pelagic bioclasts (Fig. 2). Some of them are slightly bioturbated.

Unit 5 extends from FZ 13 to the early Famennian stage. It consists of greyish and pinkish nodular to pseudo-nodular limestones and interbedded argillaceous micrite yielding poor faunas, except some tentaculite and cephalopod fragments. In the upper part of the limestones are 30 cm thick laminated blackish shales overlain by 35 cm thick laminated pinkish calcisiltites without fossils (Fig. 3c). The black shales represent the Upper Kellwasser horizon.

4.a.2. Marhouma section

The Frasnian succession is approximately 75 m thick and includes four units (Units 1 – 4). The base of this section cannot be precisely dated. Details concerning conodont contents and their biostratigraphic implications were presented in Mahboubi & Gatovsky (2014). In contrast to Ben Zireg, this section is dominated by monotonous shale deposits rich in carbonate nodules (Fig. 4).

Unit 1 belongs to the FZ 1 – 4 intervals. It consists of dark shales (Fig. 3d) with rare nodular limestones.

Unit 2 extends from the upper part of FZ 1 – 4 to the lower part of FZ 8 – 10. It is characterized by cm to dm thick, greyish to reddish, pseudo-nodular to nodular bioclastic limestones (Fig. 3e), which alternate with unfossiliferous greyish to blackish shales. The limestones are wackestone with *Styliolina* (tentaculites) coquinas; they yield phacopid trilobites and cephalopods (*Mesobeloceras* sp.) on the surface of bed MH9 (Feist, Mahboubi & Girard, 2016).

Unit 3 belongs to the FZ 8 – 10 to FZ 13 interval. It is characterized by unfossiliferous greenish and darkish shales with frequent reddish and greenish argillaceous nodular limestones (Fig. 3f). Toward the top, input of siliciclastic material increases, including mm thick intercalations of sandstone with planar-laminations. The Upper Kellwasser horizon of this section is marked by plane-laminated shales (Fig. 3g).

Unit 4 belongs to the early Famennian. It is mainly composed of dm thick diagenetic blackish argillaceous nodular limestones displaying large orthoceratids and brachiopods, and of unfossiliferous greyish laminated shales (Fig. 3h).

4. b. Facies

On the basis of differences in texture, fossil components, and lithological nature, seven sedimentary facies are identified (Figs. 2, 4). The original texture of most rocks has been obscured or obliterated during burial diagenesis, tectonic processes, or both. Indeed, micro-shear zones and stylolithes are sometimes identified within nodular limestones. Moreover, the original texture (micrite) was transformed into microsparite.

The facies description follows the distal to proximal order, from Facies 1 to Facies 7.

Laminated-black shales (F1): In both sections, finely laminated black shales are interbedded with silty shales, calcareous shales, or both. Bed thicknesses range from centimeter to few meters. In the South Marhouma section, thick layers of black shales also display *septaria* nodules, whereas such shales are less common at Ben Zireg. The faunal content is represented only by poorly preserved shelly pelagic organisms (e.g. tentaculites).

Shales, such as those at the base of Marhouma section (Fig. 3d), are usually interpreted as deposited in deep basin settings (e.g. Boulvain *et al*. 2004), probably below the storm wave-base. This facies is very common in North Africa (e.g. Ahnet and Mouydir basins (Wendt *et al.* 2006), with a high accumulation of organic matter (Boote, Clarke-Lowe & Traut,1998). They are considered as the deepest facies in the Frasnian interval.

Lithoclastic floatstone (F2): The lithoclasts mainly consist of chaotic, randomly organized angular to rounded limestone and cherty clasts (Fig. 5a, b). Carbonate clasts are composed of monomict, poorly sorted pelagic mudstones belonging to Facies 3 (see below). Lithoclasts are supported by a matrix composed of calcisiltite, clay, microsparite, and iron-hydroxide. The fossil components consist of rare pelagic ostracods (entomozoans) and tentaculite debris. Inverse grading in the lower part of some dm- thick beds are observed.

This facies was assigned to seismo-turbidites by Mutti *et al.* (1984) or megaturbidites by Cook *et al.* (1972). In our case, this facies is restricted to Unit 1 in association with convolute bedding. It corresponds to debris flows into a distal pelagic domain. This facies may also correspond to gravitational deposits that formed under low sedimentation rates and unstable depositional conditions (Rossetti & Góes, 2000). F2 is similar to facies described elsewhere in the Upper Devonian successions from the Eastern Anti-Atlas (Wendt & Belka 1991). Convolute structures associated with reworked lithoclasts can be generated by seismic shocks giving rise to downslope movements (Spalletta & Vai 1984).

Poorly fossiliferous mudstone (F3)*:* In the two sections, this facies is well represented. In the Marhouma section F3 is found in Units 1 and 3 consisting of greyish nodular cm-thick beds in shales. In the Ben Zireg section it occurs mainly in Units 3 and 5 as centimeter-thick fine-grained limestone beds or greyish nodular limestones, respectively. The matrix of this facies is micrite or microsparite. Micritic limestones lack bioturbation fabrics, whereas burrowing traces are sometimes observed in nodular limestones embedded within greyish shales. F3 is characterized by poor faunal content that is represented by pelagic organisms such as tentaculites, pelagic molluscs, entomozoans, and radiolarians. No current fabrics have been macroscopically observed in this facies.

The fine-grained matrix and rare fossils suggest low energy and open marine conditions, remaining probably under the storm wave-base (Pas *et al*., 2013; 2014a). The scarcity of biogenic activities (e.g. borings and burrows) could reflect oxygen-depleted waters (Flügel, 2004). Nodules are often of late diagenetic origin, and were presumably produced in a deep burial diagenetic environment (James & Choquette 1990).

Argillaceous pelagic wackstone (F4): This facies occurs mainly in middle Frasnian strata in both sections. It comprises cm- to dm- thick greyish to reddish limestones. Pressure solution processes commonly triggered tectonic stylolithisation. The common type of texture is wackstone with microbioclasts occurring in a patchily distribution. Thus, the matrix displays ferruginous blisters organized into isolated or grouped, concentric internal structures. The faunal content is commonly high, with tentaculites as the dominating organisms followed by entomozoans, radiolarians,

cephalopods, and pelagic mollusks (Fig. 5d). Additionally, scarce benthic faunas are represented by debris of trilobites, brachiopods, and ostracods. Bioclasts are generally poorly sorted; sometimes they are concentrated into mm-thin laminations with a random distribution of fossils and they are partially affected by bioturbation.

On the basis of the abundance of pelagic assemblages, facies F4 is interpreted as deposited in a deep-water environment, likely just below the storm wave-base (*Pas et al*., 2013; 2014a). Finely laminated biogenic detritus is interpreted as being deposited by turbidity currents or distal tempestites (*sensu* Aigner, 1985).

Diversified mudstone to wackstone (F5)*:* This facies is mostly found in the uppermost part of both sections. In the South Marhouma section, it is composed of large dark diagenetic nodules of early *triangularis* Zone age. In the Ben Zireg section, the same facies occurs within greyish nodular muddy limestones. Fossil components are dominated by nektonic faunas such as cephalopods with *Orthoceras*, mostly fragmented and poorly preserved (Fig. 5c). Pelagic organisms, radiolarians, entomozoans, and tentaculites, are less frequent. Benthic faunas are more abundant compared with Facies 4 (Fig. 5e); they are dominated by ostracods, skeletal debris of echinoderms, brachiopods, and trilobites. This facies is locally bioturbated. Early diagenetic geopetal fillings are recognized within some rotated ostracods and cephalopods coquinas.

In light of the increase in benthic faunal diversity, which is a striking feature of zones with normal oxygen concentration (Flügel, 2004), the depositional setting of this facies might be located above storm wave-base.

Lime ostracod mudstone (F6)*:* This facies is not frequent in the studied sections (samples BZ10a, BZ11, BZ13a, and MH6'). It occurs mostly in FZ 12 in the Ben Zireg section. It consists of yellowish thin bedded argillaceous limestones. The matrix is microsparite to sparite, rarely containing euhedral replacement of dolomite crystals. The bioclastic components of this mudstone consist predominantly of benthic ostracods (Fig. 5f) followed by trilobite and brachiopod fragments. Additionally, pelagic elements are limited to entomozoans, radiolarians, and unrecognized pelagic shell fragments. Micritic geopetal infillings are sometimes observed. The systematic study of benthic ostracods from acid residues revealed the presence of the suborders

Podocopida and Metacopida that can be related to the Assemblage III of Casier (2008).

The abundance of the ostracod assemblage might indicate a more proximal depositional setting compared with the previous environment, likely below the fair weather wave-base. The frequent occurrence of disarticulated ostracods may suggest para-autochthonous aggregations produced by episodic storm-induced sea floor disturbances (Schülke & Popp, 2005).

"Microbial (?) shale" (F7)*:* This facies is common in "restricted" environments in the latest Frasnian. It is exhibited in the South Marhouma section as lenticular cm- to dm-thick darkly carbonaceous to silty shale. The texture is close to the striped shale facies of Schieber (1989), with silt and mud couplets (light) alternating with carbonaceous silty shale (dark) (Fig. 6f). In petrographic thin section, the texture displays discontinuous wavy-crinkly laminae of kerogenous matter that are widely associated with framboïdal pyrites and cubic euhedral crystals (Figs. 6b, c, e). Also, terrigenous quartz grains and isolated mud fragments can be found. Imbricated flat pebbly conglomerates with argillaceous clasts are observed in bed MH26bas (Fig. 6a). Characteristic organisms are reworked benthic ostracods, rare brachiopods, and undetermined mollusk shells.

In the Ben Zireg section, the microbial (?) shale facies is observed in bed BZ15D (Uppermost FZ 13). It consists of pink laminated calcareous silty shale. The thin sections display a fine-grained matrix with abundant dolomite crystals and rare mica crystals. The wavy-crinkly laminae described above are less common (Fig. 6e) and organized into fine kerogenous units alternating with fine-grained calcareous laminae. SEM observations display tube-like shapes (Fig. 6d) occasionally forming ramiform structures and sometimes associated with rare framboidal pyrites. Fossils are very sparse, with brachiopods, benthic ostracods and tentaculite fragments.

Framboidal pyrite is commonly present in hypoxic to anoxic environments (e.g. Li Tian *et al*. 2014; Peckmann & Thiel 2004; Wignall, Newton & Brookfield, 2005) where crystallization is partly controlled by bacterial activity (e.g. Folk, 2005; Mac Lean *et al*., 2008). The association of wavy to wavy-crinkly structures with kerogen laminae has been considered resulting from the occurrence of benthic microbial (cyanobacterial?) mats (e.g. Schieber, 1986, 1989; Sur *et al*., 2006; Deb, Schieber & Chaudhuri, 2007) and coccoidal bacteria have been identified within such deposits

(Kaźmierczak, Kremer & Racki, 2012). Even if no obvious diagnostic feature of primary cyanobacterial mats (e.g. web-like texture indicator of benthic coccoidal remnants, Kremer & Kaźmierczak, 2005) were found in the studied sections, the presence of organic matter, framboidal pyrite, wavy lamination, wavy lenticular lamination with shale fragments, wavy crinkly structure and tubular structures (SEM) are strongly suggestive of the presence of microbial mats acting during the deposition of the black shales in the two sections. The presence of mud and silt couplets with locally reworked fossils and mixing of conodont assemblages indicate episodic high energy episodes attributed to storms. Such an interpretation is compatible with that of Schieber (1986, 1989) who located the depositional environment of similar shales between fair weather wave-base and average storm wave-base.

4.c. Magnetic susceptibility trends

First application of the magnetic susceptibility (MS) technique (Figs. 8, 9) provided extremely low MS values for the Frasnian and basal Famennian strata. These vary between 0.1 x 10^{-7} m^3 kg^{-1} and 8 x10^{-7} m^3 kg^{-1} at the south Marhouma section with an empirical average value of 1.9 x 10^{-7} m^3 kg^{-1}. They are even lower in the Ben Zireg anticline where they fluctuate between 3.7 x 10^{-7} m^3 kg^{-1} and 0.4 x 10^{-7} m^3 kg^{-1} with an average of 1.3 x 10^{-7} m^3 kg^{-1}. Even if the reliability of the MS measures should be tested by additional magnetic techniques (Da Silva *et al.*, 2013) to appreciate problems of re-magnetization or diagenesis, the mean values are compatible with those from other Frasnian sites. In both Algerian sections the averages of MS values are lower than those for the $MS_{marine\ standard}$ (5.5 x 10^{-7} m^3 kg^{-1}) of Ellwood *et al*. (2011) and (Da Silva, Mabille & Boulvain. 2009).This was also observed in the Carnic Alps (Pas *et al.*, 2014a) and in the Dinant Synclinorium (Pas *et al.*, 2014b) where mean values range from 0.1 to 1 x 10^{-7} m^3 kg^{-1}.

Qualitative analysis of the magnetic susceptibility suggests the same global trend with shared peaks, which are considered as isochronous (Crick *et al*. 2002), in the South Marhouma and in Ben Zireg sections (Figs. 8, 9). At Marhouma, the lower part of the section from FZ1-4 to FZ6-7 shows important fluctuation of MS value from 0 to 8 x 10^{-7} m^3 kg^{-1}. The upper part of the section, from FZ8-10 to Famennian, shows low values between 0 and 3 x 10^{-7} m^3 kg^{-1}. At Ben Zireg, the lower part of the section from FZ5 to FZ7 shows little fluctuation, between 0 and 3 x 10^{-7} m^3 kg^{-1}. In the upper

part of the section, from FZ8-10 to Famennian, the MS value remains low, between 0 and 1 x 10^{-7} m^3 kg^{-1}.

5. Discussion

5.a. Local depositional environment

Paleoenvironmental interpretations of depositional settings of Facies 1 and 3 to 7 observed in both sections (plus F2 at Ben Zireg only) allow proposing that the sediments were deposited along a low angle, mid to outer ramp profile *sensu* Wright & Burchette (1996) at regional scale (Fig. 7).

5.a.1. Ben Zireg section

The section is dominated by fine grained carbonates above a major gap in the lower Frasnian. This gap corresponds to a non-deposition and erosion? in submarine setting and was related elsewhere to bottom currents (Hüneke, 2006). The presence of such currents has not been evidenced at Ben Zireg. An outer ramp model is suggested for this area at the northern margin of Algerian Sahara (Fig. 7). In this model the deepest deposits are represented by some black shale intervals (Facies 1, Fig. 2 and 3d) and siliceous deposits with convolutes and breccias (Facies 2; Figs. 3a, 5a, b). In our model (Fig. 7), Facies 4 and 5 were emplaced below storm wave-base, as no current features were found. In Facies 4 the presence of submicrometric hydroxides may result from iron - bacteria activity (Mamet & Préat 2006). Common hardgrounds point to repeated episodes of cementation on the sea floor. The proximal part of the ramp displays accumulations of fragmented bioclasts from both benthic and pelagic communities. This is interpreted as indicating a deposition between storm wave-base and fair-weather wave-base, with an increasing amount of benthic fauna upward from Facies 5 to Facies 7 indicative of a shallowing upward trend.

5.a.2. South Marhouma section

The section is dominated by mudrocks (e.g. shales) and fine-grained carbonate deposits with open marine fauna.

From FZ 1 to 4 sedimentation resumed in autochtonous facies 1 and 3 which are the deepest facies. Facies 1 (black shales) probably indicates dysoxic to anoxic bottom conditions. Facies 2 was not found (Fig. 8). From FZ5 to FZ13 the nodular argillaceous limestones (Facies 3) with mudstone texture and rare fauna suggest distal depositional setting under quiet depositional conditions. The fine-grained bioclastic mudstone and wackstone (Facies 4 and Facies 5) with overwhelming abundance of open marine fauna (Facies 4) attest depositional setting similar to F1 and F3 but with some influence of shallow-water. Frequent occurrences of dark shales in this setting may reflect confined conditions when only organic matter was deposited upon the substrate. A shallower ramp is recognized during FZ6 – 7 and FZ12 by the increase of benthic faunal components (Facies 5). The shallowest facies herein is depicted by the occurrence of microbial (?) benthic mats (Facies 7) that are affected by storm action below the fair weather wave-base.

5.a.3. Comparison between both sections

Stratigraphic correlation between Ben Zireg and Marhouma was documented in Mahboubi *et al*. (2015). The Frasnian deposits of the South Marhouma section are nearly three times thicker than those of Ben Zireg, though mostly represented by distal shaly deposits (Facies1). We conclude in a higher sedimentation rate under subsiding basinal conditions at Marhouma. In contrast, distal carbonate deposits with minor shaly interbeds characterize Ben Zireg where Facies 3 to Facies 5 dominate. We suggest a discrete submarine rise setting on an outer ramp under low sedimentation rates. Such a depositional setting results either from submarine rise topography, or from enhanced current activity, or from a more distant location to the source areas of detrital inputs.

As a whole, the Frasnian interval at Marhouma is punctuated by several developments of hypoxic facies (black and grey shales) that are not identified in the Ben Zireg section. The absence of such facies is presumably due to the submarine rise topography or to currents activity or to a far distant location regarding the sources of detrital and biogenic materials magnetic susceptibility values are low, see below)..

5.b. Sea-level fluctuations

Integrating both lithofacies and MS data (Figs. 8 and 9), as well as data of conodont biofacies (Seddon & Sweet, 1971; Sandberg, 1976; Klapper & Barrick, 1978; Sandberg & Ziegler 1979) 'recently published in both studied sections (Mahboubi & Gatowsky, 2014; Mahboubi *et al*., 2015), we tentatively interpret environmental changes through middle and late Frasnian times in terms of bathymetrical variation. However, we are aware that changes in bathymetry might not be the sole cause of fluctuations in the percentage of conodont genera in succeeding populations (Belka & Wendt 1992).

5.b.1. Early Frasnian

During the early Frasnian (FZ1 – 4), the Marhouma section displays a regressive trend with an upward change from facies 1 to 3 and fluctuating MS values (Fig. 8). This trend is in contradiction to the transgressive trend recorded in North America (Fig. 10) at that time. It could be related to the specific location of the Marhouma section where abundant fine-grained siliciclastic inputs from the emerging West African Shield might have obscured the eustatic signal.

5.b.2. Middle Frasnian

Between FZ 5 and the beginning of FZ 8/10, both sections display instabilities of MS and lithofacies values (Fig. 8 and 9). During this interval, at Marhouma, slight shifts of MS values roughly reflect concomitant shifts in lithofacies. In contrast, at Ben Zireg, shifts in both MS and lithofacies values, though discernible, are less pronounced with lower amplitudes in their maximum excursions. MS values, in particular, that vary between 0 and 8 units at Marhouma, are much lower at Ben Zireg with a shift from 1 to 3 units and as such being almost insignificant. In parallel, variations in succeeding lithofacies are more vigorous with shifts from F1 to F6 at Marhouma, whereas these are restricted to F2+3 and F4 at Ben Zireg. Mean prevalence of F4 in both sections along with a poorly documented decrease in MS values coincide with biofacies indicators available at Ben Zireg that shift temporarily from shallower Po-Ic (*Polygnathus-Icriodus*) in FZ 6 to deeper Po between FZ 7 and the beginning of FZ8/10 before returning to Po-Ic thereafter (Mahboubi *et al*., 2015).

During the middle Frasnian the global trend is transgressive (Johnson & Sandberg, 1988; Sandberg *et al.*, 1992). In the nearby Tafilalt region this trend is perceptible since FZ8 (Dopieralska, Belka, & Walczak, 2016) and culminates at the end of FZ 10

(Fig. 10). This trend is likewise to be observed at Ben Zireg. At Marhouma, the global transgressive trend begins in the lower part of FZ6 to FZ10 but a marked regressive event occurred at the transition from during FZ6-7.

5.b.3. Late Frasnian

MS values remain constantly very low throughout the late Frasnian without any significant changes at the Upper Kellwasser level in particular.

During the early FZ11 there is a regressive event followed by a transgressive peak in the late FZ 11. This transgressive peak is characterized by a significant extension of deep sea lithofacies, associated with biofacies Po-Pa (*Polygnathus-Palmatolepis*) dominated conodont associations. This signal is most obvious at Ben Zireg (Mahboubi *et al*., 2015), whereas, at Marhouma, the paucity of available conodont record prevents to confirm the slight deepening of the sedimentary setting there (Mahoubi & Gatowsky, 2014). The curve of Ben Zireg remarkably coincides with the curves obtained in Euramerica and in theTafilalt (Fig. 10). At Marhouma, only the transgressive peak is clearly recorded. Dopieralska, Belka, & Walczak (2016) emphasize the importance of the *semichatovae* transgression with the highest positive shift in εNd values within FZ 11. This event has earlier been described from Euramerica where it is characterized by the sudden spread of *Palmatolepis semichatovae* in FZ 11 (Sandberg *et al*. 1992; Sandberg, Morrow & Ziegler, 2002). This species has not been established in the studied sections, but the obvious transgressive episode recorded within FZ 11 at both Marhouma and Ben Zireg may most likely correspond to this event. As a whole, the *semichatovae* transgression is evidenced in the Saharian Platform.

During FZ 12 shallower environments reappear between Facies 5 and Facies 6 at Ben Zireg, and between Facies 1 and Facies 7 at Marhouma. Biofacies in both sections clearly indicate a shallowing trend with predominance of Po-An (*Polygnatus-Ancyrodella*) (Mahoubi & Gatowsky, 2014; Mahboubi *et al*., 2015). This regressive trend was also identified in Euramerica and in the Tafilalt (Fig. 10).

At the top of FZ 12 and the transition between FZ 12 and FZ 13 the hypoxic Lower Kellwasser horizon (LKW), usually occurring elsewhere, is not developed in its typical shale facies in our sections. Litho- and biofacies indicate a sudden increase in bathymetry followed up by fluctuations of lithofacies that average increase of water depth up to the Upper Kellwasser (UKW) horizon. Indicators of concomitant biofacies

appear to be somewhat contradictory, as they remain constant in prevalence of Pa-Po and Pa at Ben Zireg but return to shallower signals at Marhouma (Mahboubi & Gatovsky 2014, Mahboubi *et al*. 2015). The increase in bathymetry observed in our sections is in accordance with that of Euramerica and Tafilalt (Fig. 10). Dopieralska, Belka, & Walczak (2016) also identified regressive trends coinciding in particular with the Lower and Upper Kellwasser extinction events at the FZ 12/13 transition and at the top of FZ 13 respectively. At Ben Zireg and Marhouma the LKW deposits are not lithologically recognized and precisely located; any regressive trend occurs slightly earlier, still within FZ12 when biofacies Po-An (*Polygnathus-Ancyrodella*) biofacies dominates. This anomaly might perhaps be introduced by local palaeoecological factors, in relation to the absence of the Lower Kellwasser horizon, as thereafter "normal" transgressive conditions are progressively emplaced matching the global sea-level trend.

The Upper Kellwasser horizon is characterized by its typical hypoxic facies at Ben Zireg. Bathymetric criteria point to a relative highstand of sea-level at the beginning of the event followed up by a marked decrease of water depth until its top with development of Pa-An biofacies (Mahboubi *et al*., 2015) and occurrence of possible "microbial shales" (F7). In contrast, at Marhouma, the drop in sea level seems to start earlier when F7 and Po-Ic (Polygnatus-Icriodus) are present at the beginning of the presumed Upper Kellwasser (Mahboubi & Gatowsky, 2014). Consequently, it cannot be excluded that the equivalent of the Upper Kellwasser event starts a little earlier at Marhouma than considered by Mahboubi & Gatovsky (2014). At top of FZ 13 the major regression during the UKW event occurs both at Ben Zireg and Marhouma and is in accordance with the results of Dopieralska, Belka, & Walczak (2016) and Johnson & Sandberg (1988).

5.b.4. Summary

The bathymetric curves in the Saharian Platform display a continuing sea-level rise through the middle Frasnian punctuated by a first regression at the base of FZ11, but with a minor regression at FZ6 at Marhouma. During the late Frasnian in Euramerica, this global transgressive event achieves its highest stand from the top of FZ 11 to FZ 13, intercalated by two regressions prior to and succeeding the Lower Kellwasser (LKW) event. This is matched by the recently established curve based on Nd isotopic data presented by Dopieralska, Belka, & Walczak (2016). Coincident

results on bathymetric evolution obtained by an independent method, data gathered from neighboring southeastern Moroccan terrains, are of importance for the comparative interpretation of the curve established in SW Algeria (Fig. 10).

As expected, Frasnian sections of SW Algeria display a similar sea-level evolution through mid- and late Frasnian times than in neighboring parts of Gondwana (Morocco). Differences in deposits (absence or presence of LKW), in timing (changes in sea-level occuring later in SW Algeria than elsewhere) and amplitude of changes in both litho- and biofacies between sites might result from effects of locally different, tectonically driven rates in subsidence. In addition, sampling bias cannot be excluded in highly condensed portions such as in the lower part of the Ben Zireg section, or, on the contrary, when conodonts are rather scarce in deposits with high sedimentation rates as occur in the early through middle Frasnian in the Marhouma trough (Mahboubi *et al*., 2015).

6. Conclusions

The investigated sections through the middle and late Frasnian are composed of seven marine lithofacies that vary in time and duration throughout the successions. These lithofacies are organized along a very low angle, mid to outer ramp at the scale of the western part of the Saharian platform. Condensed carbonate sedimentation on discrete highs prevail in the North (Ben Zireg) whereas abundant shaly deposits occur in the South (Marhouma). Vertical facies changes are most perceptible at Marhouma both during the early middle and the latest Frasnian where rapid shifts between deep and shallow lithofacies occur. During the late middle and early upper Frasnian more stable conditions with the deposition of bioclastic mud- and wackstones prevail. Conversely, at Ben Zireg, these latter conditions characterize the condensed middle and earliest late Frasnian succession. A deepening occurred in the upper part of FZ 11, followed up by a marked shallowing at the beginning of FZ 12 and an average deepening up to the Upper Kellwasser. The latter is marked in both sections by a regressive-transgressive cycle.

Provisional measurements of magnetic susceptibility provided very low values. Shifts are more pronounced with rapid variations in the lower part of the middle Frasnian, remaining constantly rather low thereafter up to the Frasnian/Famennian boundary in both sections. In particular, no significant shift is available at the equivalent levels of

the Kellwasser event. Further, more detailed and bed-by-bed measurements are necessary to reconsider MS trends comparatively.

A sea-level curve, tentatively established mainly on data from Ben Zireg matches the "standard" curves already provided at a world scale. Especially, the middle Frasnian transgression, the lower FZ11 regression, the the *semichatovae* transgression within FZ 11, the lower FZ12 regression, the upper FZ13 transgression and Upper Kellwasser regression are clearly evidenced in the Saharian platform.

Acknowledgements

Algerian authorities are thanked to provide permission to access to the field. We acknowledge Tadjedinne Hassen, Kada Abess and Brigitte Meyer-Berthaud for their help in the field. The first field trip was supported by the ANR Palasiafrica (ANR-08-JCJC-0017). A. Mahboubi is grateful to Jean-Louis Bodinier for his funding (IRSES MEDYNA grant) for one month. This is publication ISE-M 2017-XXX.

References

AIGNER, T. 1985. Storm Depositional Systems. Dynamic Stratigraphy in Modern and Ancient Shallow-Marine Sequences. Springer-Verlag, Berlin, *Lecture Note in Earth Sciences* **3**, 1-174

ALEKSEEV, A.S., KONONOVA L.I., NIKISHIN A.M. 1996. The Devonian and Carboniferous of the Moscow Syneclise (Russian Platform): stratigraphy and sea-level changes. *Tectonophysics* **268**,149-168.

BECKER, R.T., GRADSTEIN, F.M & HAMMER, O. 2012. The Devonian Period. In *The geologic time scale 2012* (eds Gradstein, F., Ogg, J., Schmitz, M. & Ogg, G.), Elsevier, 559-601.

BELKA, Z. & WENDT, J.1992. Conodont biofacies pattern in the Kellwasser Facies (upper Frasnian/lower Fammenian) of the eastern Anti−Atlas, Morocco. *Palaeogeography, Palaeoclimatolology, Palaeoecology* **91**, 143-173

BENDELLA, M. & MEHADJI, A.O. 2014. Depositional environment and Ichnology (Nereites ichnofacies) of the Late Devonian Sahara region (SW Algeria). *Arabian Journal of Geology* **7**, 1-14.

BOOTE, D.R.D., CLARK-LOWES, D.D. & TRAUT M.W. 1998. Palaeozoic petroleum systems of North Africa. In *Petroleum Geology of North Africa* (eds D.S. Macgregor, R.T.J. Moody & D.D. Clark-Lowes). Journal of the Geological Society of London, Special Publication **132**, 7-68.

BOULVAIN, F. , CORNET, P., DA SILVA, A.C., DELAITE, G., DEMANY B., HUMBLET, M., RENARD, M. & COEN-AUBERT, M. 2004. Reconstructing atoll-like mounds from the Frasnian of Belgium. *Facies* **50**, 313–326.

CASIER, J.C. 2008. Résumés des communications et guide de l'excursion consacrée aux ostracodes du Dévonien Moyen et Supérieur de Dinant. In *22 th Réunions des Ostracologistes de Langue Française*, Institut Royal des Sciences Naturelles de Belgique, Département de Paléontologie, Bruxelles, pp 1-88.

CHEN, D. & TUCKER, M.E. 2003. Palaeokarst and its implication for the extinction event at the Frasnian–Famennian boundary (Guilin, south China). *Journal of the Geological Society of London* **161**, 895-898.

COOK, H.E., MCDANIEL, P.N., MOUNTJOY, E.W. & PRAY, L.C. 1972. Allochthonous carbonate debris flows at Devonian bank ("reef') margins, Alberta, Canada. *Bulletin of Canadian Petroleum Geology* **20**, 439–497.

CRICK, R.E., ELLWOOD, B.B., HLADIL, .J, EL HASSANI, A., HROUDA, F. & CHLUPAC, I. 2001. Magnetostratigraphy susceptibility of the Pridolian–Lochkovian (Silurian–Devonian) GSSP (Klonk, Czech Republic) and coeval sequence in Anti-Atlas Morocco. *Palaeogeography, Palaeoclimatololgy, Palaeoecology* **167**, 73-100.

DA SILVA, A. C., DE VLEESCHOUWER, D. et al. 2013. Magnetic susceptibility as a high-resolution correlation tool and as a climatic proxy in Paleozoic rocks-merits and pitfalls: examples from the Devonian in Belgium. *Marine and Petroleum Geology* **46**, 173-189.

DA SILVA, A.C., MABILLE, C. & BOULVAIN, F. 2009. Influence of sedimentary setting on the use of magnetic susceptibility: examples from the Devonian of Belgium. *Sedimentology* **56**,1292-1306.

DEB, S.P., SCHIEBER, J. & CHAUDHURI, A.K. 2007. Microbial mat features, mudstones of the Mesoproterozoic Somanpalli Group, Pranhita-Godavari Basin, India. In *Atlas of Microbial Mat Features Preserved within the Siliciclastic Rock Record* (eds Schieber, J., Bose, P.K., Eriksson, P.G., Banerjee, S., Jadavpur, S.S., Altermann, W. & Catuneanu, O.). Elsevier, Amsterdam, **2**, 171-180.

DONZEAU, M. 1974. L'arc Anti-Atlas-Ougarta (Sahara Nord occidental, Algérie, Maroc). Comptes Rendus de l'Académie des Sciences, Paris, (II), **278**, 417-420.

DOPIERALSKA, J., BELKA, Z. & WALCZAK, A. 2016. Nd isotope composition of conodonts: An accurate proxy of sea-level fluctuations. *Gondwana Research* **34**, 284-295.

DUNHAM, R.J. 1962. Classification of carbonate rocks according to depositional texture. In *Classification of Carbonate Rocks* (ed Ham, W.E.). American Association of Petroleum Geologists, Memoir **1**, 108-121.

ELLWOOD, B.B., TOMKIN, J.H., EL HASSANI, A., BULTYNCK, P., BRETT, C.E., SCHINDLER, E., FEIST, R. & BARTHOLOMEW, A.J. 2011. A climate-driven model and development of a floating point time scale for the entire Middle Devonian Givetian Stage: A test using magnetostratigraphy susceptibility as a climate proxy. *Palaeogeography, Palaeoclimatololgy, Palaeoecology* **304**, 85-95.

FEIST, R., MAHBOUBI, A. & GIRARD, C. 2016. New Late Devonian phacopid trilobites from Marhouma, SW Algerian Sahara, *Bulletin of Geosciences* **91**, 243-259.

FLÜGEL, E. 2004. *Microfacies of carbonate rocks. Analysis, Interpretation and Application*. Springer-Verlag , Berlin, Heildelberg, NewYork, pp 1-984.

FOLK, R.L., 2005. Nannobacteria and the formation of framboidal pyrite: Textural evidence. *Journal of Earth Systems in Sciences* **114**, 369-374.

GÖDDERTZ, B. 1987. Devonische Goniatiten aus SW-Algerien und ihre stratigraphische Einordnung in die Conodonten-Abfolge. *Palaeontographica Abtelung A* **197**:127-220.

HALLAM, A. & WIGNALL, P.B. 1999. Mass extinctions and sea-level changes. *Earth Science Review* **48**, 217-250.

HAQ, B.U. & SCHUTTER, S.R. 2008. A Chronology of Paleozoic Sea-Level Changes. *Science* **322**, 64-68.

JAMES, N.P. & CHOQUETTE, P.W. 1990. Limestone - The meteoric diagenetic environment. In *Diagenesis* (eds Mc Ilreath, I.A. & Morrow, D.W.). *Geosciences Canada* **4**, 35-73.

JOHNSON, J. G., KLAPPER, G. & SANDBERG, C. A.1985. Devonian eustatic fluctuations in Euramerica. *Geological Society of America Bulletin* **96**, 567-87.

JOHNSON, J.G. & SANDBERG, C.A. 1988. Devonian eustatic events in the Western United States and their biostratigraphic responses. In *Devonian of the World* (eds McMillan, N.J., Embry, A.F. & Glass, D.J.). *Canadian Petroleum Geology, Calgary* **14**,171-178.

KAŹMIERCZAK, J., KREMER, B. & RACKI, G., 2012. Late Devonian marine anoxia challenged by benthic cyanobacterial mats. *Geobiology* **10**, 371-383.

KLAPPER, G. & BARRICK, J.E. 1978. Conodont ecology: pelagic versus benthic. *Lethaia* **11**, 15-23.

KLAPPER, G. & KIRCHGASSER, W.T. 2016. Frasnian Late Devonian conodont biostratigraphy in New York: graphic correlation and taxonomy. *Journal of Paleontology* **90**, 525-554.

KREMER, B. & KAŹMIERCZAK, J. 2005. Cyanobacterial mats from Silurian black radiolarian cherts: phototrophic life at the edge of darkness? *Journal of Sedimentary Resarch* **75**, 897-906.

LI TIAN, TONG J., ALGEO, T.J., SONG, H., CHU, D., SHI, L. & BOTTJER, D.J. 2014. Reconstruction of Early Triassic ocean redox conditions based on framboidal pyrite from the Nanpanjiang Basin, South China. *Palaeogeogeography, Palaeoclimatolology, Palaeoecology* **412**, 68-79.

Mac LEAN, L.C.W., TYLISZCZAK, T., GILBERT, P.U.P.A., ZHOU, D., PRAY, T.J., ONSTOTT, T.C. & SOUTHAM, G. 2008. A high-resolution chemical and structural study of framboidal pyrite formed within a low-temperature bacterial biofilm. *Geobiology* **6**, 471-480.

MAHBOUBI, A. & GATOVSKY, Y. 2014. Late Devonian conodonts and event stratigraphy in northwestern Algerian Sahara. *Journal of African Earth Sciences* **101**, 322-332.

MAHBOUBI, A., FEIST, R., CORNÉE, J.-J., MEHADJI, A.O. & GIRARD, C. 2015. Frasnian (Late Devonian) conodonts and environment at the northern margin of the Algerian Sahara platform: the Ben Zireg section. *Geological Magazine* **152**, 844-857.

MAMET, B. & PRÉAT, A. 2006. Iron-bacterial mediation in Phanerozoic red limestones: State of the art. *Sedimentary Geology* **185**, 147-157.

MUTTI, E., LUCCHI, F.R., SEGURET, M. & ZANZUCCHI, G. 1984. Seismoturbidites: A new group of resedimented deposits. *Marine Geology* **55**, 103-116.

NARKIEWICZ, M. 1988. Turning points in sedimentary development in the Late Devonian in southern Poland. In *Devonian of the World* (eds McMillan, N.J., Embry, A.F. & Glass, D.J.). *Canadian Petroleum Geology*, *Calgary*, 14, 619–636.

PAREYN, C. 1961. Les Massifs Carbonifères du Sahara Sud-Oranais. *Publications du Centre de Recherches Sahariennes*, série Géologie, Paris, 1–324.

PAS, D., DA SILVA, A.C., CORNET, P., BULTYNCK, P., KÖNIGSHOF, P. & BOULVAIN, F. 2013. Sedimentary development of a continuous Middle Devonian to Mississippian section from the fore-reef fringe of the Brilon Reef Complex (Rheinisches Schiefergebirge, Germany). *Facies* **59**, 969-990.

PAS, D., DA SILVA, A.C., SUTTER, T., KIDO, E., BULTYNCK, P.,PONDRELLI, M., CORRADINI, C., DEVLEESCHOUWER, X., DOJEN , C. & BOULVAIN, F. 2014a. Insight into the development of a carbonate platform through a multi-disciplinary approach: a case study from the Upper Devonian slope deposits of Mount Freikofel (Carnic Alps, Austria/Italy*). International Journal of Earth Sciences* **103**, 519-538.

PAS, D., DA SILVA, A.C., DEVLEESCHOUWER, X., DE VLEESCHOUWER, D., LABAYE, C., CORNET, P., MICHEL, J., BOULVAIN, F. 2014b. Sedimentary development and magnetic susceptibility evolution of the Frasnian in Western

Belgium (Dinant Synclinorium, La Thure section). *Geological Society of London*, Special Publication **414**, 15-36.

PECKMANN, J. & THIEL, V. 2004. Carbon cycling at ancient methane–seeps. *Chemical Geology* **205**, 443–467.

PETTER, G. 1952. Dévonien moyen et supérieur. In *Les chaines d'Ougarta et la Saoura* (eds Alimen, H.D., Le Maitre, D., Menchikoff, N., Petter, G. & Poueyto, A.). 19th Congrès géologique International, Alger, 62–74.

PETTER, G. 1959. Goniatites Dévoniennes du Sahara. Service de la carte géologique de l'Algérie, Alger, 313 pp.

ROSSETTI, D.F. & GÓES, A.M. 2000. Deciphering the sedimentological imprint of paleoseismic events: an example from the Aptian Codó Formation, northern Brazil. *Sedimentary Geology* **135**, 137-156.

SANDBERG, C.A. 1976. Conodont biofacies of Late Devonian *Polygnathus styriatus* Zone in western United States. In *Conodont Paleoecology* (ed. C. R. Barnes), pp. 171–86. Montreal: Geological Association of Canada, Special Paper no. 15.

SANDBERG, C.A. & ZIEGLER, W. 1979. Taxonomy and biofacies of important conodonts of Late Devonian styriacus Zone, United States and Germany. *Geology and Palaeontology*, 13, 173-212.

SANDBERG, C.A., ZIEGLER, W., DREESEN, R. & BUTLER, J.L. 1992. Conodont biochronology, biofacies, taxonomy, and event stratigraphy around middle Frasnian Lion Mudmound (F2h), Frasnes, Belgium. *Courier Forschunginstitut Senckenberg* **150**, 1–87.

SANDBERG, C.A., MORROW, J.R. & ZIEGLER, W. 2002. Late Devonian sea-level changes, catastrophic events, and mass extinctions. *Special papers - Geological Society of America*, 473-488.

SCHIEBER, J. 1986. The possible role of benthic microbial mats during the formation of carbonaceous shales in shallow Proterozoic basins. *Sedimentology* **33**, 521-536.

SCHIEBER, J. 1989. Facies and origin of shales from the Mid-Proterozoic Newland Formation, Belt basin, Montana, USA. *Sedimentology* **36**, 203-219.

Schülke, I. & Popp, A. 2005. Microfacies development, sea-level change, and conodont stratigraphy of Famennian mid- to deep platform deposits of the Beringhauser Tunnel section (Rheinisches Schiefergebirge, Germany). *Facies* **50**, 647-664.

SEDDON, G. & SWEET, W.C. 1971. An ecologic model for conodonts. *Journal of Paleontology* **45**, 869-880.

SPALLETTA, C. & VAI, G.B. 1984. Upper Devonian intraclast parabreccias interpreted as seismites. *Marine Geology* **55**, 133-144.

SUR, S., SCHIEBER, J. & BANERJEE, S. 2006. Petrographic observations suggestive of microbial mats from Rampur Shale and Bijaigarh Shale, Vindhyan basin, India. *Journal of Earth System Science* **115**, 61-66.

WENDT, J. & BELKA, Z. 1991. Age and depositional environment of Upper Devonian (early Frasnian to early Famennian) black shales and limestones (Kellwasser facies) in the eastern Anti-Atlas, Morocco. *Facies* **25**, 51-89.

WENDT, J., KAUFMANN, B., BELKA, Z., KLUG, C. & LUBESEDER, S. 2006. Sedimentary evolution of a Palaeozoic basin and ridge system: the Middle and Upper Devonian of the Ahnet and Mouydir (Algerian Sahara). *Geological Magazine* **143**, 269-299.

WEYANT, M. 1988. Relationship between Devonian and Carboniferous strata near the northern confines of the Bechar basin, Algeria. *Courier Forschunginstitut Senckenberg* **100**, 235-241

WIGNALL, P.B., NEWTON, R. & BROOKFIELD, M.E. 2005. Pyrite framboid evidence for oxygen-poor deposition during the Permian–Triassic crisis in Kashmir. *Palaeogeography, Palaeoclimatology, Palaeoecology* **216**, 183-188.

WRIGHT, V. P. & BURCHETTE, T. P. 1996. Shallow-water carbonate environments. In *Sedimentary Environments: Processes, Facies, and Stratigraphy* (ed. H. G. Reading), pp. 325–94. Oxford: Blackwell Science.

Figure captions

Fig. 1. (**a**) Location of South Marhouma section (Ougarta basin) and Ben Zireg section (Bechar basin) in NW Algeria (photograph from Google Earth). (**b**) Investigated section in the Saoura region (after Petter, 1959). (**c**) Investigated section in the Ben Zireg anticline (after Pareyn, 1961).

Fig. 2. Lithological column with relative abundance of fossil components and facies fabrics of the Ben Zireg section. Conodont zones from Mahboubi et al. (2015). Lithostratigraphic units: (Unit 1) ochre cherty limestones with soft-deformations, (Unit 2) massive micritic limestones, (Unit 3) ferruginous limestones, (Unit 4) pseudo nodular argillaceous limestones, (Unit 5) nodular limestones. Abbreviations: Hg, Hard ground; M, Mudstone; W, Wackestone; P, Packstone; F, Floatstone; FZ, Frasnian Zone (after Klapper & Kirchgasser, 2016).

Fig. 3. Lithofacies. (**a**) Convolute laminations (Ben Zireg). (**b**) Thin-bedded, upper Frasnian micritic limestones (Ben Zireg). (**c**) Detail of the Upper Kellwasser bed in the Ben Zireg section with a thin layer of black shales (red arrow) superseded by laminated pinkish calcisiltic shale (black arrow). (**d**) Black shales (Marhouma). (**e**) Alternating pseudonodular limestone beds and grey shales (Marhouma section). (**f**) Interbedded argillaceous micritic nodules (Marhouma Formation). (**g**) Upper Kellwasser bed in the South Marhouma section with laminated black to pinky shales. (**h**) Dm-thick diagenetic limestones and black shales from early Famennian strata of the Marhouma section.

Fig. 4. Lithological column with relative abundance of fossil components and facies fabrics of the South Marhouma section. Conodont zones from Mahboubi & Gatovsky (2014). Lithostratigraphic units: (Unit1) dark shales, (Unit 2) bioclastic nodular/pseudonodular limestones-grey shales, (Unit 3) nodular muddy limestones-greenish/darkish shales, (Unit 4) Diagenetic limestones/black shales. Abbreviations: Hg, Hard ground; M, Mudstone; W, Wackestone; P, Packstone, L.*tr*., Lower *triangularis*; FAM, Famennian; FZ, Frasnian Zone.

Fig. 5. Facies of the depositional environments of the South Marhouma section and the Ben Zireg section. Scale (yellow bar) is 1mm. (**a**) Facies F2, outer ramp deposit: reworked mudstone layers in the Ben Zireg section (bed BZ2B). (**b**)) Facies F2, outer ramp deposit: microscopic view (bed BZ1C). (**c**) Facies F6, mid-outer ramp deposit: lime mudstone with cephalopod bioclasts (bed MH34. (**d**) Facies F4, outer ramp deposit: pelagic argillaceous wackstone displaying distinct lamination by parallel arrangement of tentaculite coquinas (bed MH10). (**e**) Facies F6, outer ramp deposit: diversified wackestone with bioclasts consisting of abundant brachiopod shells (bed MH32). (**f**)) Facies F6, mid ramp deposit: fine-grained mudstone with benthic ostracods (bed BZ10B). Abbreviations: br, brachiopod; go, goniatite; ort, orthoceras; os, ostracod; pa, parabreccia; ra, radiolarian; tr, trilobite; te, tentaculite

Fig. 6. Facies F7, mid ramp deposits, latest Frasnian at South Marhouma and Ben Zireg sections. (**a**) Flat-pebble conglomerate fabric (bed MH26bas). (**b**) SEM image of kerogenous laminae (wavy-crinkly structures) (bed MH29). (**c**, **e**) Kerogenous laminae. Note that these structures are more abundant in the South Marhouma samples (picture b, bed MH29) compared to the Ben Zireg sample (picture e, bed BZ15D). (**d**) SEM image of tube-like structures (black arrows, bed BZ15D) associated with framboidal pyrite (white arrow). (**f**) Finely-laminated striped shale displaying graded silt-mud couplets (bed MH30).

Fig. 7. Sedimentary model in NW Algeria during the Frasnian period (South Marhouma and Ben Zireg sections). This model shows a mid to outer ramp setting with lateral distribution of facies from the most proximal setting (F7) to the the most distal (F1). SWB, Storm Wave-Base; FWWB, Fair Weather Wave-Base.

Fig. 8. Magnetic susceptibility evolution, facies change, and sea-level fluctuations through the Frasnian in the South Marhouma section. FZ: Frasnian Zones, LKW: Lower Kellwasser, UKW: Upper Kellwasser.

Fig. 9. Magnetic susceptibility evolution, facies change, and sea-level fluctuations through the Frasnian in the Ben Zireg section. FZ: Frasnian Zones, LKW: Lower Kellwasser, UKW: Upper Kellwasser.

Fig. 10. Comparison of sea-level fluctuations from Euramerica and North Africa through the Frasnian stage. FZ (Frasnian Zones) after Klapper & Kirchgasser (2016), relative duration of conodont Zones are from Becker, Gradstein & Hammer (2012). In grey anoxic events. UKW: Upper Kellwasser; LKW: Lower Kellwasser; FAM: Famennnian.

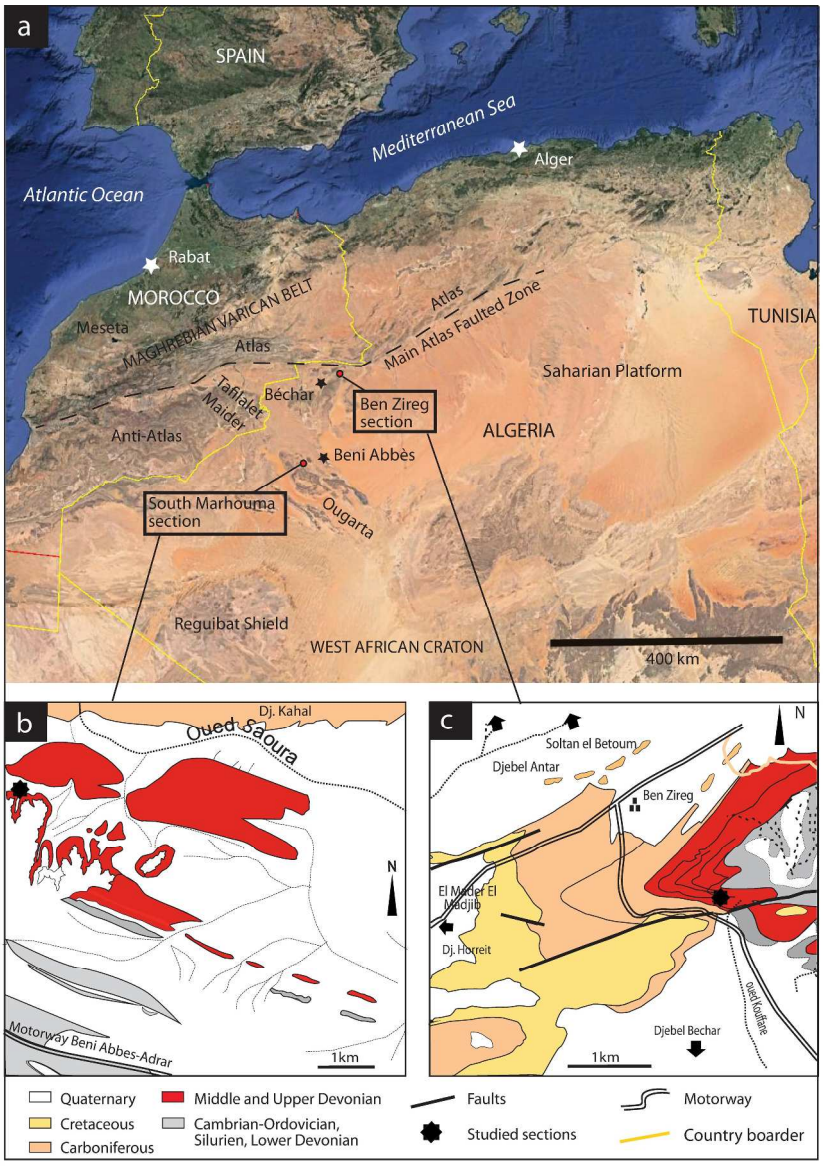

Mahboubi et al., Fig. 1

Fig. 1. (a) Location of South Marhouma section (Ougarta basin) and Ben Zireg section (Bechar basin) in NW Algeria (photograph from Google Earth). (b) Investigated section in the Saoura region (after Petter, 1959). (c) Investigated section in the Ben Zireg anticline (after Pareyn, 1961).

290x408mm (300 x 300 DPI)

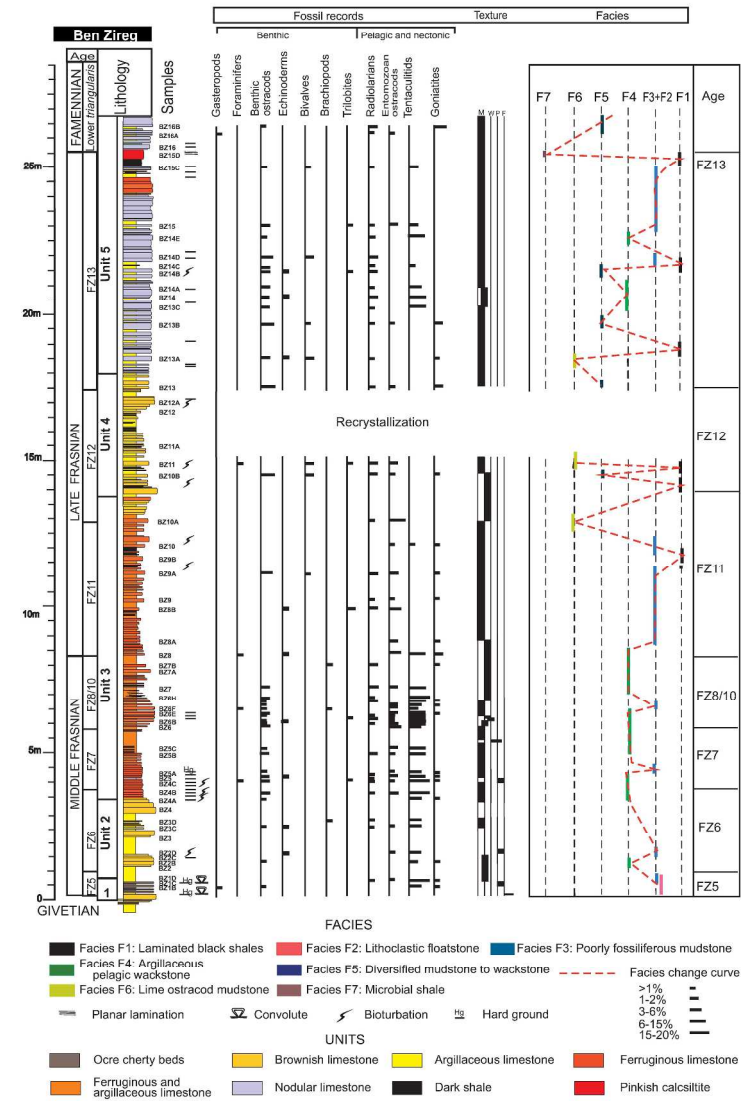

Fig. 2. Lithological column with relative abundance of fossil components and facies fabrics of the Ben Zireg section. Conodont zones from Mahboubi et al. (2015). Lithostratigraphic units: (Unit 1) ochre cherty limestones with soft-deformations, (Unit 2) massive micritic limestones, (Unit 3) ferruginous limestones, (Unit 4) pseudo nodular argillaceous limestones, (Unit 5) nodular limestones. Abbreviations: Hg, Hard ground; M, Mudstone; W, Wackestone; P, Packstone; F, Floatstone; FZ, Frasnian Zone (after Klapper & Kirchgasser, 2016).

283x463mm (300 x 300 DPI)

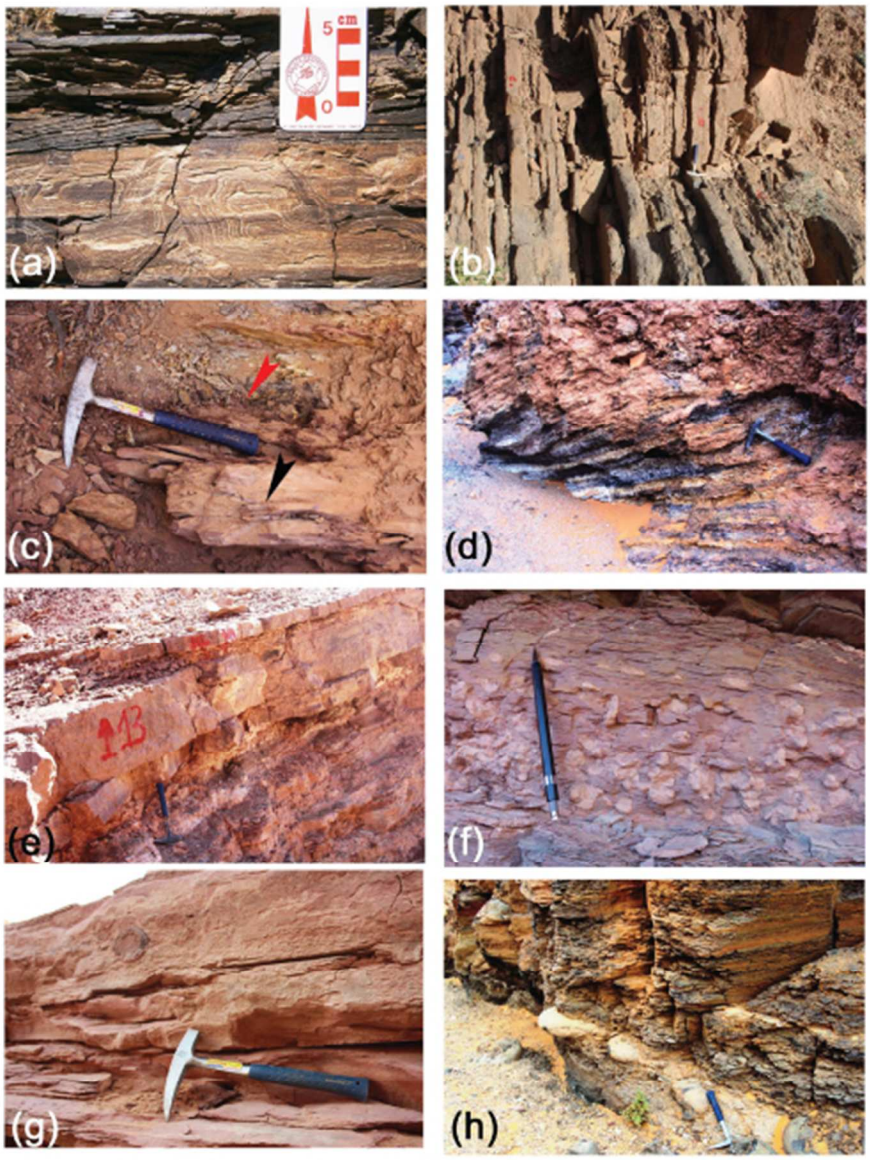

Fig. 3. Lithofacies. (a) Convolute laminations (Ben Zireg). (b) Thin-bedded, upper Frasnian micritic limestones (Ben Zireg). (c) Detail of the Upper Kellwasser bed in the Ben Zireg section with a thin layer of black shales (red arrow) superseded by laminated pinkish calcisiltic shale (black arrow). (d) Black shales (Marhouma). (e) Alternating pseudonodular limestone beds and grey shales (Marhouma section). (f) Interbedded argillaceous micritic nodules (Marhouma Formation). (g) Upper Kellwasser bed in the South Marhouma section with laminated black to pinky shales. (h) Dm-thick diagenetic limestones and black shales from early Famennian strata of the Marhouma section.

190x239mm (72 x 72 DPI)

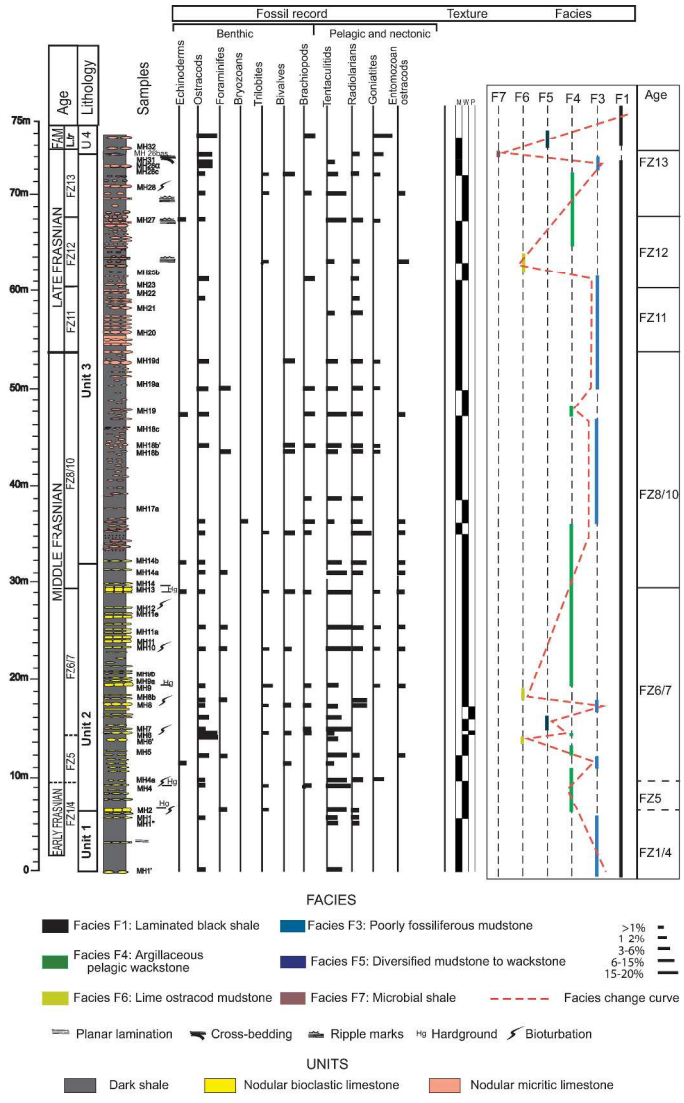

Mahboubi et al., Fig. 4

Fig. 4. Lithological column with relative abundance of fossil components and facies fabrics of the South Marhouma section. Conodont zones from Mahboubi & Gatovsky (2014). Lithostratigraphic units: (Unit1) dark shales, (Unit 2) bioclastic nodular/pseudonodular limestones-grey shales, (Unit 3) nodular muddy limestones-greenish/darkish shales, (Unit 4) Diagenetic limestones/black shales. Abbreviations: Hg, Hard ground; M, Mudstone; W, Wackestone; P, Packstone, L.tr., Lower triangularis; FAM, Famennian; FZ, Frasnian Zone.

270x439mm (300 x 300 DPI)

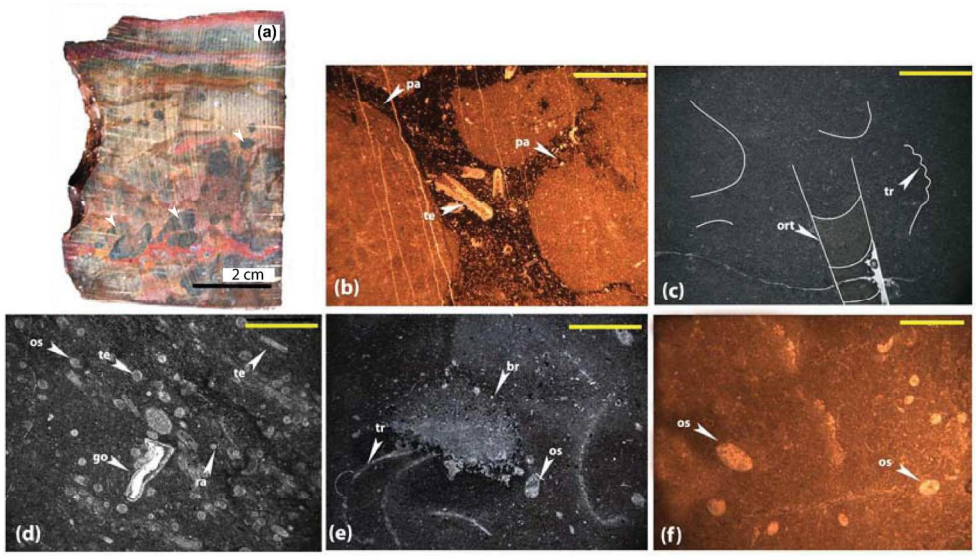

Mahboubi et al. Fig. 5

Fig. 5. Facies of the depositional environments of the South Marhouma section and the Ben Zireg section. Scale (yellow bar) is 1mm. (a) Facies F2, outer ramp deposit: reworked mudstone layers in the Ben Zireg section (bed BZ2B). (b)) Facies F2, outer ramp deposit: microscopic view (bed BZ1C). (c) Facies F6, mid-outer ramp deposit: lime mudstone with cephalopod bioclasts (bed MH34. (d) Facies F4, outer ramp deposit: pelagic argillaceous wackstone displaying distinct lamination by parallel arrangement of tentaculite coquinas (bed MH10). (e) Facies F6, outer ramp deposit: diversified wackestone with bioclasts consisting of abundant brachiopod shells (bed MH32). (f)) Facies F6, mid ramp deposit: fine-grained mudstone with benthic ostracods (bed BZ10B). Abbreviations: br, brachiopod; go, goniatite; ort, orthoceras; os, ostracod; pa, parabreccia; ra, radiolarian; tr, trilobite; te, tentaculite

167x148mm (300 x 300 DPI)

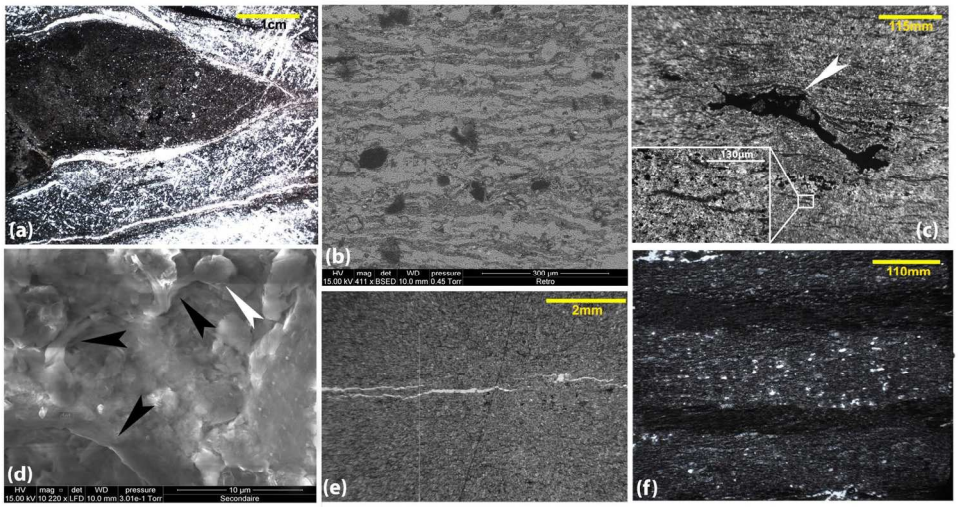

Mahboubi et al;, fig. 6

Fig. 6. Facies F7, mid ramp deposits, latest Frasnian at South Marhouma and Ben Zireg sections. (a) Flat-pebble conglomerate fabric (bed MH26bas). (b) SEM image of kerogenous laminae (wavy-crinkly structures) (bed MH29). (c, e) Kerogenous laminae. Note that these structures are more abundant in the South Marhouma samples (picture b, bed MH29) compared to the Ben Zireg sample (picture e, bed BZ15D). (d) SEM image of tube-like structures (black arrows, bed BZ15D) associated with framboidal pyrite (white arrow). (f) Finely-laminated striped shale displaying graded silt-mud couplets (bed MH30).

168x133mm (300 x 300 DPI)

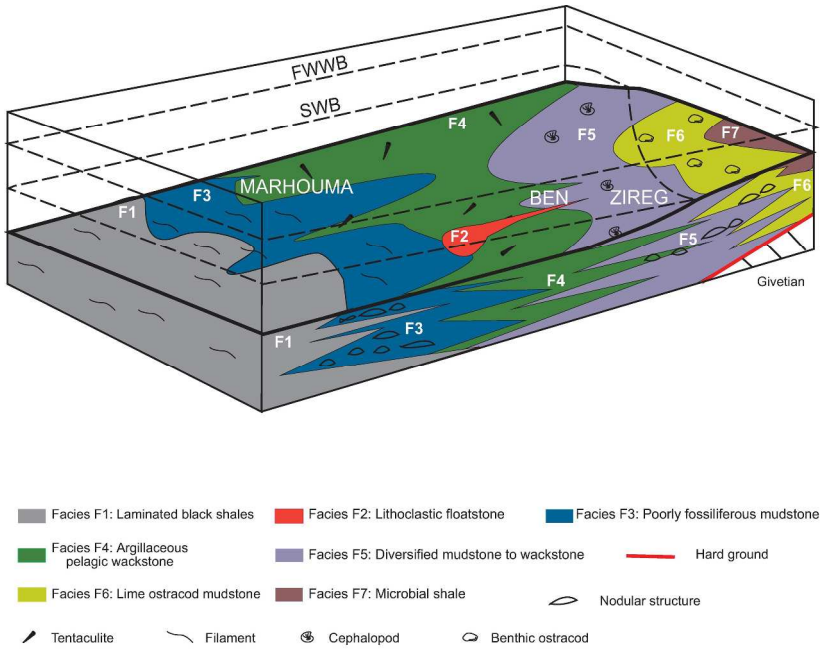

Mahboubi et al. Fig. 7

Fig. 7. Sedimentary model in NW Algeria during the Frasnian period (South Marhouma and Ben Zireg sections). This model shows a mid to outer ramp setting with lateral distribution of facies from the most proximal setting (F7) to the the most distal (F1). SWB, Storm Wave-Base; FWWB, Fair Weather Wave-Base.

257x378mm (300 x 300 DPI)

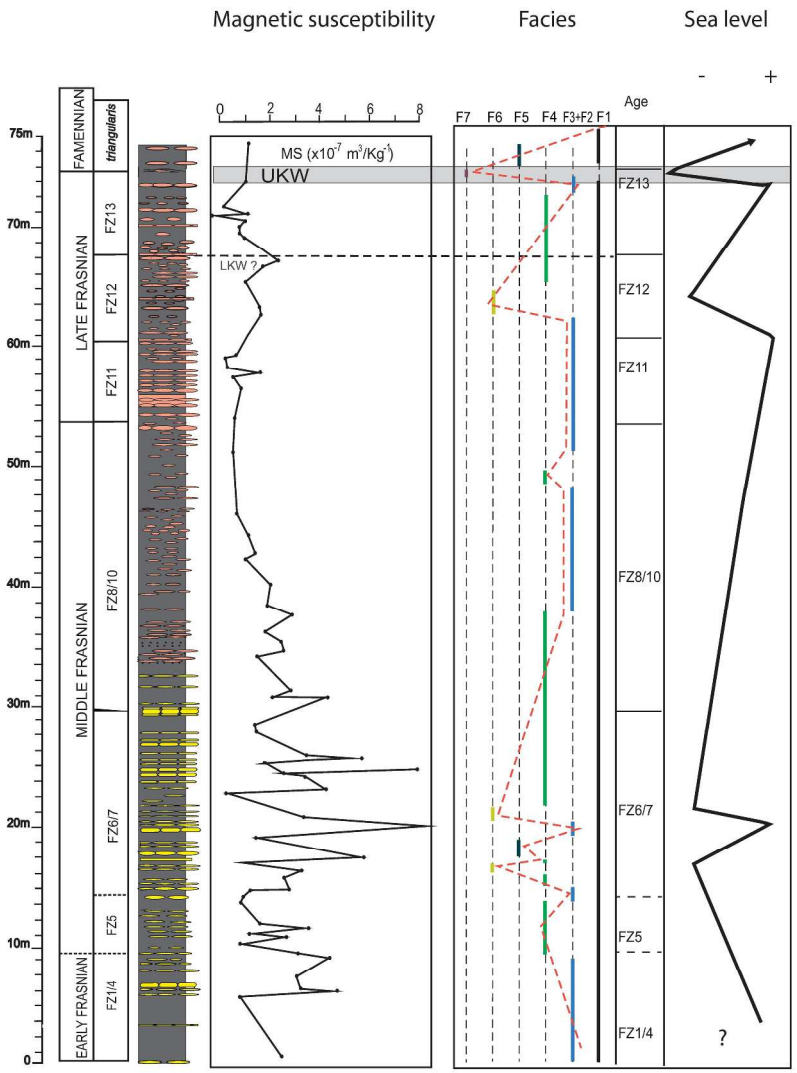

Mahboubi et al., Fig. 8

Fig. 8. Magnetic susceptibility evolution, facies change, and sea-level fluctuations through the Frasnian in the South Marhouma section. FZ: Frasnian Zones, LKW: Lower Kellwasser, UKW: Upper Kellwasser.

260x384mm (300 x 300 DPI)

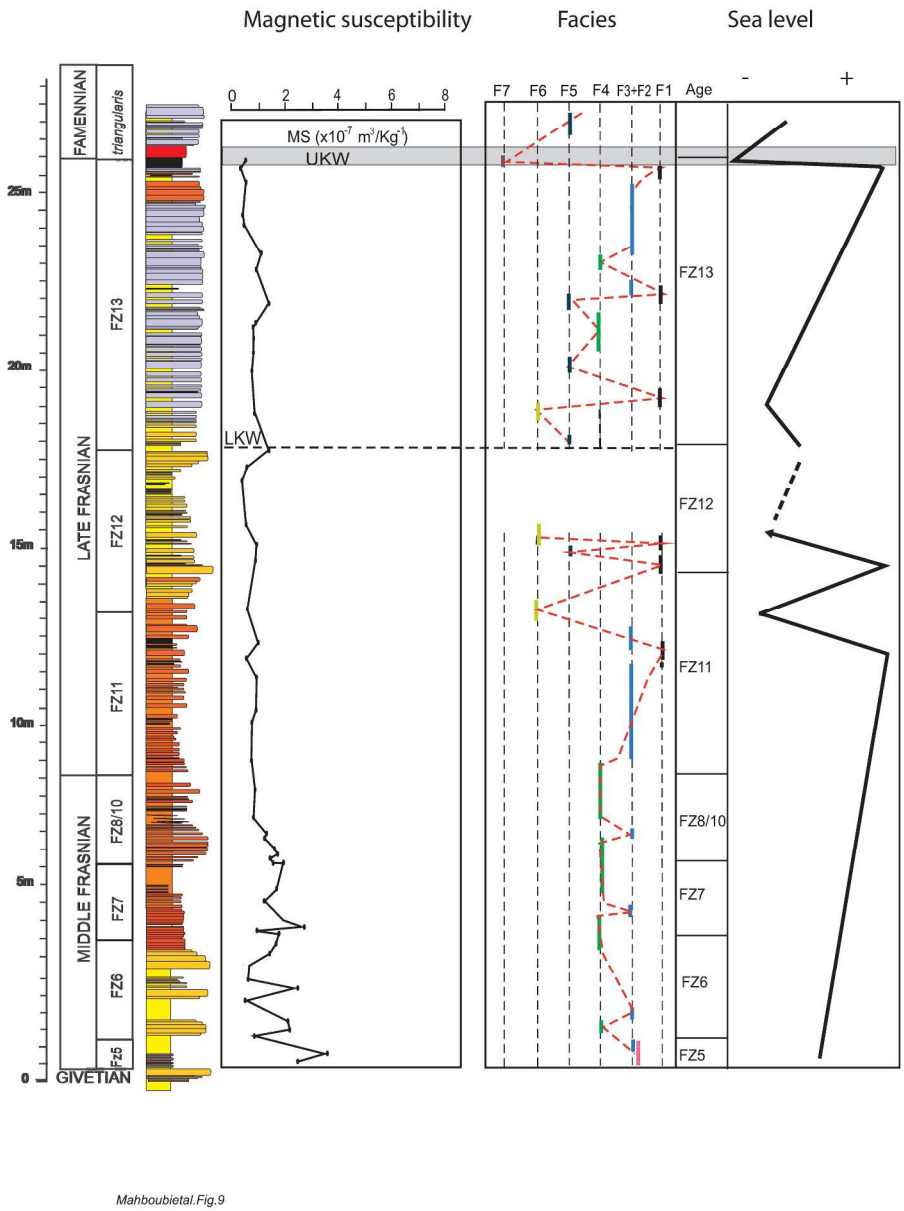

Fig. 9. Magnetic susceptibility evolution, facies change, and sea-level fluctuations through the Frasnian in the Ben Zireg section. FZ: Frasnian Zones, LKW: Lower Kellwasser, UKW: Upper Kellwasser.

238x320mm (300 x 300 DPI)

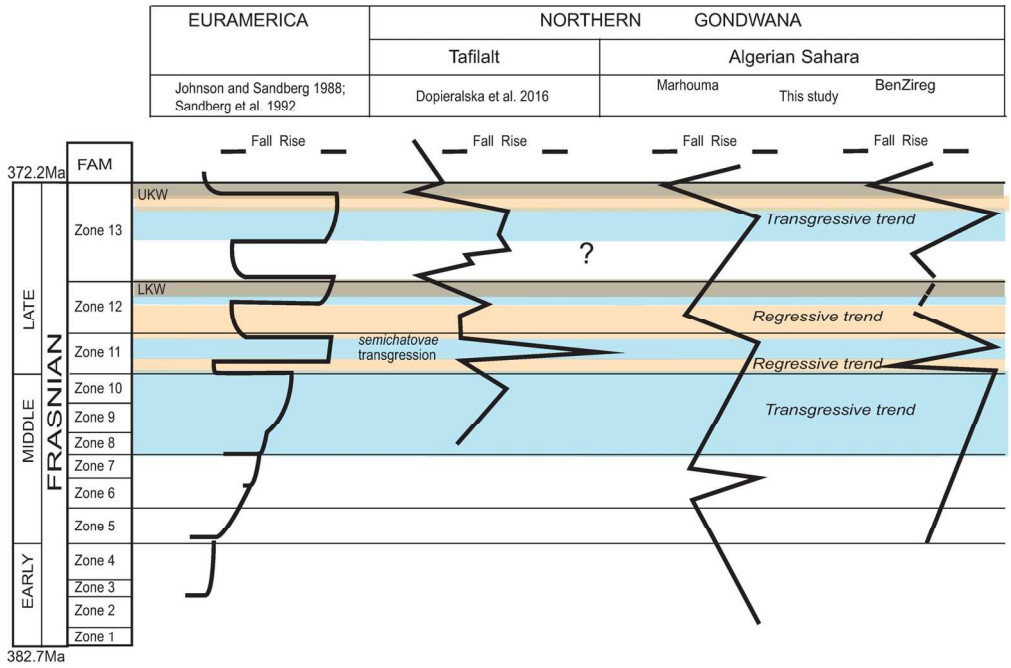

Fig. 10. Comparison of sea-level fluctuations from Euramerica and North Africa through the Frasnian stage. FZ (Frasnian Zones) after Klapper & Kirchgasser (2016), relative duration of conodont Zones are from Becker, Gradstein & Hammer (2012). In grey anoxic events. UKW: Upper Kellwasser; LKW: Lower Kellwasser; FAM: Famennnian.

147x123mm (300 x 300 DPI)